Time Distribution of Adsorption Energies, Local Monolayer Capacities, and Local Isotherms on Heterogeneous Surfaces by Inverse Gas Chromatography

N. A. Katsanos* and E. Arvanitopoulou

Physical Chemistry Laboratory, University of Patras, 26500 Patras, Greece

F. Roubani-Kalantzopoulou and A. Kalantzopoulos

Department of Chemical Engineering, National Technical University, 15780 Zografou, Greece

Received: October 12, 1998; In Final Form: December 7, 1998

A new inverse gas chromatographic methodology is introduced to measure local (homogeneous) adsorption energies, ϵ, local monolayer capacities, c^*_{max}, and adsorption isotherms, $\theta_i(p,T,\epsilon)$ for probe gases on heterogeneous solid surfaces in the presence of nitrogen as carrier gas. The method does not depend on analytical solutions of the classical integral equation comprising the adsorption energy distribution function $f(\epsilon)$ as unknown, nor on numerical solutions and estimations from this equation, using powerful computers. It simply uses a time function of the chromatographic peaks obtained by short flow-reversals of the carrier gas, combined with the local isotherm model of Jovanovic. All three adsorption parameters ϵ, c^*_{max}, and $\theta_i(p,T,\epsilon)$ mentioned above can be calculated as a function of the experimental time and refer to instantaneous equilibration of the probe gases with the heterogeneous surface, with different kinds of active sites *i* being involved at different times. The kinetic physicochemical parameters for the adsorption phenomenon are also included for the gas/solid systems studied, being C_2H_4/ZnO, C_2H_4/PbO, C_3H_6/PbO, and C_3H_6/$CaCO_3$. A comparison of the adsorption energy values found for these systems with heats of adsorption reported elsewhere is impermissible, since the latter refer to overall values and not to local values as in the present method. However, some literature values seem rather comparable to the present ones.

Introduction

Inverse gas chromatography has the stationary phase of the system as the main object of investigation. Usually, the same procedures as in direct gas chromatography (GC) are employed, but the results are used to derive properties of the stationary phase. The main source of information obtained experimentally is the broadening of the chromatographic elution peaks, and the analysis of their statistical moments. However, classical GC systems are not in true equilibrium during the retention period, needing extrapolation to infinite dilution and zero carrier gas flow rate to approximate true equilibrium parameters. An acceptable precision of the quantities determined is a difficult, if not impossible, task in many cases.

During the last decade, inverse gas−solid chromatography was employed for characterizing heterogeneous solids by calculating adsorption energy distribution functions from retention volume data, the subject being recently reviewed.[1] One is impressed by the various ways used to overcome the difficulty or rather impossibility of obtaining an analytical solution of the classical integral equation

$$\Theta(p,T) = \int_0^\infty \theta_i(p,T,\epsilon)\, f(\epsilon)\, d\epsilon \qquad (1)$$

where $\Theta(p,T)$ is the overall experimental adsorption isotherm, unless approximations are used for the local adsorption isotherm $\theta_i(p,T,\epsilon)$, and/or the adsorption energy distribution function $f(\epsilon)$. Difficulties like this led scientists to turn into numerical solutions and estimations[2−7] of $f(\epsilon)$, which open another way to the problem solution, but these need powerful computers not easily available everywhere.

An inverse gas chromatographic tool is the reversed-flow gas chromatography (RF-GC) technique for physicochemical measurements, which dismisses the carrier gas from doing the work, and "appoints" the gaseous diffusion process in its place. The carrier gas performs only the sampling procedure to measure the gas-phase concentration of an analyte A at a certain position as a function of time. The RF-GC technique has been used for measurement of various physicochemical quantities, some recent ones being collected in a review.[1] It is worth mentioning the simultaneous determination of six parameters pertaining to the deposition of air pollutants on solid surfaces, including rate constants of surface and gaseous reactions, and experimental isotherms.[8] The only physicochemical assumptions concerning the gas/solid interactions are that all parameters measured directly or calculated indirectly refer to elementary steps at equilibrium. It seems that RF-GC offers a new pathway to the determination of adsorption energies, monolayer capacities, and local isotherms of gaseous substances on heterogeneous solid surfaces, as distributed over the instrumental time, i.e., time measured from the moment of introduction of the gas under study into the solid bed and continued as long as the chromatographic detector records substance concentrations. The method is described in the present paper and exemplified by presenting representative results.

Theory

The experimental arrangement, on which the following theoretical analysis is based, has been published before[8] and is repeated in Figure 1 for convenience. Injecting a small amount of the adsorbate gas or vapor A (0.5−1 cm^3 under atmospheric

10.1021/jp984041h CCC: $18.00
Published on Web 02/03/1999

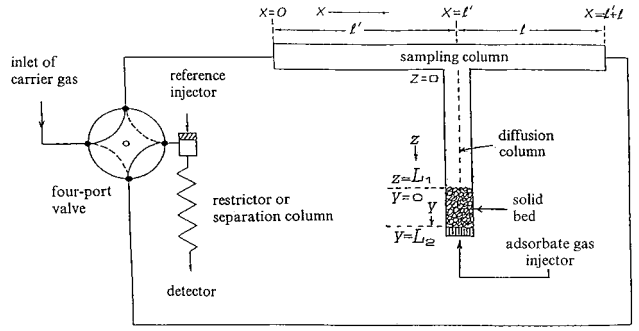

Figure 1. Schematic representation of the columns and gas connections showing the principle for using the reversed-flow technique as an inverse gas chromatography tool.

pressure) at the end $y = L_2$ of the solid bed and making repeated flow-reversals of short duration (10−60 s) of the carrier gas (air or N_2) by means of the four-port valve, one obtains in the recorder a series of narrow, symmetrical *sample peaks* of considerable height H above the continuous chromatographic signal, depending on the time t at which the flow-reversal was made. This procedure has been described in detail earlier[9] giving also examples of sample peaks in Figure 2 of ref 9. The only difference in the present work is that the diffusion column contains a bed of solid particles at its closed end.

A mathematical model[1,8] is based on (a) two mass balances for the gaseous concentrations c_y (mol/cm^3) and c_z (mol/cm^3) of the analyte A in the regions y and z of the diffusion column, respectively, (b) the rate of change of the adsorbed concentration c_s (mol/g), and (c) the isotherm for the local adsorbed equilibrium concentration c_s^* (mol/g) of A on the solid, at time t:

$$c_s^* = \frac{n_s}{a_s}\delta(y - L_2) + \frac{a_y}{a_s}k_1\int_0^t c_y(\tau)\,d\tau \tag{2}$$

where n_s is the amount of A adsorbed initially and $\delta(y - L_2)$ is the Dirac delta function. The term "local" in the above relation means with respect to time t, i.e., involving not all adsorption energy sites, but only those active at time t. This time distinguishing is attributed to different rates of adsorption with time connected in some unknown way to the adsorption energy. The expression "equilibrium concentration" for c_s^* means microscopically reversible, not a statical one.

This simple experimental way of determining the local with respect to time isotherm directly over a wide range of gaseous concentrations $c_y(\tau)$ (τ = dummy variable for time), without specifying *a priori* an isotherm equation, was introduced in 1995.[10]

The solution of the mathematical model described above[1] under (a), (b), and (c) leads to the following equations for the peak height H, the gaseous concentration c_y above the solid at $y = 0$ of the solid bed, and the local adsorbed equilibrium concentration c_s^* of the adsorbate A as a function of time t:

$$H^{1/M} = \sum_{i=1}^{4} A_i \exp(B_i t) \tag{3}$$

$$c_y = \frac{\nu L_1}{gD_1}\sum_{i=1}^{4} A_i \exp(B_i t) \tag{4}$$

$$c_s^* = \frac{a_y}{a_s}k_1\frac{\nu L_1}{gD_1}\sum_{i=1}^{4}\frac{A_i}{B_i}[\exp(B_i t) - 1] \tag{5}$$

where M is the response factor of the detector, g is the calibration factor of the chromatographic detector[10] in cm (peak height)/(mol cm^{-3}), D_1 is the diffusion coefficient of A in section z of the diffusion column, ν is the corrected linear flow velocity of the carrier gas, L_1 is the length of section z of the diffusion column, a_y is the cross sectional area of the void space in the solid bed, a_s is the amount of solid per unit length of bed (g/cm), and k_1 (s^{-1}) is the adsorption rate constant of A on the surface. All above quantities (except M, ν, L_1, a_y, and a_s) contained in eqs 3−5, including the pre-exponential factors A_i and the coefficients of time B_i, are calculated by nonlinear regression analysis with a PC program in GW-BASIC[1,8] from the experimental pairs H, t.

The concentration c_s^* of eq 5 at time t is that which would be established if a microscopically reversible equilibrium existed between the gas phase concentration $c_y(\tau)$ of eq 2 and the adsorption sites active at that particular time. The question naturally arising is: what is the mean adsorption energy and the other characteristics of the adsorption sites that are active at time t? To find this, one can start from the equilibrium differential isotherm already published:[10]

$$\frac{\partial c_s^*}{\partial c_y} = \frac{a_y}{a_s}k_1\frac{\sum_{i=1}^{4} A_i \exp(B_i t)}{\sum_{i=1}^{4} A_i B_i \exp(B_i t)} \tag{6}$$

In addition, an isotherm model is required and a fairly general one for our purposes is that of Jovanovic:[11]

$$\theta(p,T,\epsilon) = 1 - \exp(-Kp) \tag{7}$$

going over to Langmuir isotherm in middle pressures and to a linear form at low pressures. The K is Langmuir's constant given by the relation[7]

$$K = K^0(T)\exp(\epsilon/RT) \tag{8}$$

where R is the gas constant, and $K^0(T)$ is described by statistical mechanics[12] as

$$K^0 = \frac{h^3}{(2\pi m)^{3/2}(kT)^{5/2}}\frac{\upsilon_s(T)}{b_g(T)} \tag{9}$$

k being the Boltzmann constant, m the molecular mass, h the Planck constant, $b_g(T)$ the partition function for the rotations and vibrations of the free gas molecule, and $\upsilon_s(T)$ the partition function of the adsorbed molecule over all possible quantum states. As a low temperature approximation, we adopt that $\upsilon_s(T) \approx b_g(T)$, as was done before.[7]

Although the physical foundations of eq 7 have been criticized,[13] this isotherm gives a good representation of experimental gas adsorption and behaves correctly at a wide range of surface coverages. An exhaustive numerical investigation of the differences in the behavior of the Jovanovic isotherm compared with that of Langmuir[14] led to the conclusion that, for the system krypton−pyrex, there is nothing to choose between the two and both give very similar values of the monolayer capacities. Also, Sircar[15] used the Jovanovic isotherm as the kernel $\theta(\epsilon,T,p)$ in the integral equation (1) to calculate the energy distribution function $f(\epsilon)$, and this resulted in the same form of $f(\epsilon)$ as that obtained by using the Langmuir isotherm as the kernel. Only the variance of the calculated

function was affected. Jaroniec et al.[16] investigated the possibility of extending the Jovanovic equation to multilayer adsorption on heterogeneous surfaces. In discussing numerical methods of evaluating the adsorption energy distribution from eq 1, Rudzinski and Everett[17] describe the application of Laplace transforms to the Jovanovic equation used as the local adsorption isotherm $\theta(p,T,\epsilon)$, not only to monolayer but also to multilayer adsorption. Landman and Montroll[18] investigated the energy distribution function that converts the Langmuir local isotherm into the Jovanovic equation. The temperature dependence of this function shows that the picture of surface heterogeneity given by the Jovanovic and the Langmuir isotherms becomes more and more different as the temperature increases. The short review above regarding the Jovanovic isotherm (eq 7) justifies its use in the present work to calculate adsorption energies of gases on solids by inverse GC in the form of RF-GC.

The fraction of the surface covered at a given time t is denoted as $\theta_t = c_s^*/c_{max}^*$, c_{max}^* being now the local with respect to time monolayer capacity, i.e., the maximum adsorbed concentration of the gaseous substance A on the collection of sites being active at time t and having a mean adsorption energy ϵ. Instead of the partial pressure of A, p, we write c_yRT, considering A an ideal gas. Therefore, according to eq 7

$$\theta_t = \frac{c_s^*}{c_{max}^*} = 1 - \exp(-KRTc_y) \tag{10}$$

From this, one can calculate the first two derivatives of θ_t with respect to c_y, keeping in mind that c_{max}^* is a constant for each collection of sites i, active at time t:

$$\frac{\partial\theta_t}{\partial c_y} = \frac{1}{c_{max}^*}\frac{\partial c_s^*}{\partial c_y} = KRT\frac{c_{max}^* - c_s^*}{c_{max}^*} \tag{11}$$

$$\frac{\partial^2\theta_t}{\partial c_y^2} = \frac{1}{c_{max}^*}\frac{\partial^2 c_s^*}{\partial c_y^2} = -(KRT)^2\frac{c_{max}^* - c_s^*}{c_{max}^*} \tag{12}$$

Dividing the two above equations, using also eq 8, we find

$$-\frac{\partial^2 c_s^*}{\partial {c_y}^2}\Big/\frac{\partial c_s^*}{\partial c_y} = KRT = RTK^0\exp(\epsilon/RT) \tag{13}$$

Thus, the calculation of the two derivatives $\partial c_s^*/\partial c_y$ and $\partial^2 c_s^*/\partial {c_y}^2$ leads directly to the mean value of ϵ for the sites i being responsible for the adsorption at time t, since everything else on the right-hand side (rhs) of eq 13 is known. The first derivative is given by eq 6, while the second derivative of eq 13 is found from eq 3 as a function of time t:

$$\frac{\partial^2 c_s^*}{\partial {c_y}^2} = \frac{a_y}{a_s}k_1\frac{gD_1}{\nu L_1}\times \left\{\frac{1}{\sum_i A_iB_i\exp(B_it)} - \frac{[\sum_i A_i\exp(B_it)][\sum_i A_iB_i^2\exp(B_it)]}{[\sum_i A_iB_i\exp(B_it)]^3}\right\} \tag{14}$$

From eqs 6 and 14, one calculates as a function of time the left-hand side (lhs) of eq 13 and from this the value of ϵ at any chosen time t of the experiment, by means of the obvious relation derived from eq 13:

$$\epsilon = RT\left[\ln\left(-\frac{\partial^2 c_s^*}{\partial {c_y}^2}\Big/\frac{\partial c_s^*}{\partial c_y}\right) - \ln(RT) - \ln K^0\right] \tag{15}$$

From eq 11, one finds

$$c_{max}^* = c_s^* + \frac{\partial c_s^*}{\partial c_y}\Big/KRT \tag{16}$$

and thus the local monolayer capacity of each collection of active sites is computed, knowing c_s^* from (5), $\partial c_s^*/\partial c_y$ from (6), and KRT from (13).

The local (with respect to time) adsorption isotherm $\theta_t = c_s^*/c_{max}^*$ for each time t, is found by simple rearrangement of eq 16.

Calculations

The calculations of the physicochemical quantities pertaining to the adsorption energy on heterogeneous surfaces starts from the diffusion band of RF-GC experiments, comprising the values of the pairs H, t. From these, the time coefficients B_1, B_2, B_3, and B_4 of eq 3 are extracted, together with the rate constant k_1 and the calibration factor g, by means of a PC program published as the Appendix of ref 1. The other quantities needed, ν, a_y, a_s, D_1, L_1, R, k, h, T, and m, are known from literature or from conventional measurements. Introducing all the above quantities into a simple PC program based on eq 9 for K^0, eqs 6 and 14 for $\partial c_s^*/\partial c_y$ and $\partial^2 c_s^*/\partial {c_y}^2$, respectively, and eqs 5, 15, and 16, one finds the values of ϵ, c_{max}^*, and θ_t in the simplest possible way and for several times (within the frame of the experimental time t). The c_y value corresponding to these values can simply be calculated by means of eq 4.

Instead of the above procedure, one may use the compact PC program in GW-BASIC available as Supporting Information in the present work to calculate directly from the experimental pairs H, t the values of ϵ, c_{max}^*, θ_t, and c_y, together with the adsorption parameter k_1, the desorption rate constant k_{-1}, a possible first-order surface reaction rate constant k_2, the deposition velocity V_d and the reaction probability γ of the probe gas on the solid surface, the effective diffusion coefficient D_1 of the probe gas into the carrier gas, and the calibration factor of the detector g. All calculations of the above quantities, except for ϵ, c_{max}^*, θ_t, and c_y are based on ref 1. The values M (of eq 3), a_y, a_s, ν, and L_1 needed in eqs 4, 6, and 14, and some other known data are entered into the appropriate INPUT lines of the program, together with the range of times t_1 and t_2 in which ϵ, c_{max}^*, θ_t, and c_y are calculated and printed. A step of 2 min is arbitrarily set in the program, but this can be changed to smaller distances between calculation times, or eqs 4−6 and 14−16 may be used with the PC program MATHEMATICA 3 to plot ϵ, c_{max}^*, θ_t, and c_y vs t between the two limits of the experimental time with a number of plot points of, e.g., 3000.

Experimental Section

The chemicals, apparatus, and procedure were those described elsewhere.[8] The $CaCO_3$ was a Penteli marble (Greece) and its analysis has been given before.[19]

Results and Discussion

The method described in the present work to measure directly the adsorption energies, the local monolayer capacities, and the

TABLE 1: Time Distribution of Adsorption Energies (ϵ), Local Monolayer Capacities (c^*_{max}), and Local Adsorption Isotherms (θ_t) for Two Probe Gases (C_2H_4, C_3H_6) and Three Solids (ZnO, PbO, $CaCO_3$) at 323.2 K

	ϵ, kJ/mol				c^*_{max}, mol/g				θ_t			
	C_2H_4		C_3H_6		C_2H_4		C_3H_6		C_2H_4		C_3H_6	
time, min	ZnO	PbO	PbO	$CaCO_3$	ZnO	PbO	PbO	$CaCO_3$	ZnO	PbO	PbO	$CaCO_3$
6	88.3	88.4	88.8		1.18×10^{-6}	2.20×10^{-6}	8.68×10^{-8}		0.521	0.456	0.240	
8	90.9	89.7	89.6		1.72×10^{-6}	3.57×10^{-6}	1.87×10^{-7}		0.676	0.568	0.442	
10	96.6	91.7	90.7		2.03×10^{-6}	4.70×10^{-6}	2.84×10^{-7}		0.866	0.675	0.547	
12	97.1	95.0	92.2	89.4	2.69×10^{-6}	5.48×10^{-6}	3.67×10^{-7}	2.53×10^{-8}	0.877	0.801	0.638	0.144
14	91.0	106.2	94.4	88.9	4.28×10^{-6}	5.81×10^{-6}	4.29×10^{-7}	5.18×10^{-8}	0.690	0.970	0.738	0.266
16	88.1	96.6	98.4	88.6	6.42×10^{-6}	8.16×10^{-6}	4.66×10^{-7}	8.54×10^{-8}	0.551	0.844	0.861	0.332
18	86.0	92.4	109.4	88.6	9.43×10^{-6}	1.14×10^{-5}	4.97×10^{-7}	1.24×10^{-7}	0.434	0.710	0.980	0.382
20	84.3	90.1	97.2	88.7	1.40×10^{-5}	1.53×10^{-5}	6.87×10^{-7}	1.66×10^{-7}	0.332	0.610	0.836	0.426
22	82.7	88.5	93.8	89.0	2.15×10^{-5}	1.98×10^{-5}	8.98×10^{-7}	2.10×10^{-7}	0.239	0.532	0.731	0.468
24	81.0	87.2	91.7	89.4	3.58×10^{-5}	2.49×10^{-5}	1.14×10^{-6}	2.54×10^{-7}	0.157	0.469	0.648	0.509
26	78.9	86.2	90.2	89.9	7.11×10^{-5}	3.07×10^{-5}	1.42×10^{-6}	2.96×10^{-7}	0.085	0.417	0.580	0.550
28	75.3	85.4	89.0	90.5	2.53×10^{-4}	3.72×10^{-5}	1.73×10^{-6}	3.36×10^{-7}	0.026	0.373	0.521	0.592
30	74.6	84.6	88.0	91.2	3.29×10^{-4}	4.45×10^{-5}	2.09×10^{-6}	3.73×10^{-7}	0.021	0.334	0.468	0.636
32	77.0	84.0	87.1	92.1	1.40×10^{-4}	5.29×10^{-5}	2.52×10^{-6}	4.06×10^{-7}	0.052	0.300	0.420	0.683
34	77.8	83.3	86.2	93.2	1.07×10^{-4}	6.26×10^{-5}	3.03×10^{-6}	4.34×10^{-7}	0.072	0.269	0.373	0.733
36	78.1	82.7	85.5	94.7	9.56×10^{-5}	7.39×10^{-5}	3.66×10^{-6}	4.57×10^{-7}	0.084	0.240	0.329	0.788
38	78.2	82.1	84.7	96.8	9.23×10^{-5}	8.75×10^{-5}	4.46×10^{-6}	4.74×10^{-7}	0.090	0.213	0.286	0.850
40	78.2	81.6	83.9	100.3	9.31×10^{-5}	1.04×10^{-4}	5.51×10^{-6}	4.84×10^{-7}	0.093	0.187	0.243	0.920
42	78.2	81.0	83.1	119.2	9.64×10^{-5}	1.25×10^{-4}	6.98×10^{-6}	4.90×10^{-7}	0.093	0.162	0.202	0.998
44	78.0	80.3	82.2	100.1	1.02×10^{-4}	1.53×10^{-4}	9.15×10^{-6}	5.80×10^{-7}	0.090	0.138	0.161	0.917
46	77.8	79.7	81.2	96.6	1.09×10^{-4}	1.90×10^{-4}	1.27×10^{-5}	6.78×10^{-7}	0.087	0.115	0.121	0.847
48	77.6	78.9	79.9	94.6	1.19×10^{-4}	2.43×10^{-4}	1.96×10^{-5}	7.85×10^{-7}	0.082	0.093	0.081	0.787
50	77.3	78.1	78.0	93.1	1.30×10^{-4}	3.26×10^{-4}	3.83×10^{-5}	9.01×10^{-7}	0.077	0.071	0.043	0.732
52	77.0	77.0	72.6	92.0	1.44×10^{-4}	4.71×10^{-4}	2.78×10^{-4}	1.03×10^{-6}	0.071	0.051	0.006	0.684
54	76.7	75.6	76.6	91.1	1.61×10^{-4}	7.89×10^{-4}	6.35×10^{-5}	1.16×10^{-6}	0.065	0.031	0.028	0.639
56	76.4	73.0	78.5	90.3	1.81×10^{-4}	2.01×10^{-3}	3.24×10^{-5}	1.31×10^{-6}	0.059	0.012	0.056	0.598
58	76.0	70.4	79.4	89.6	2.06×10^{-4}	5.20×10^{-3}	2.34×10^{-5}	1.47×10^{-6}	0.052	0.005	0.080	0.560
60	75.7	74.2	80.0	89.0	2.37×10^{-4}	1.28×10^{-3}	1.92×10^{-5}	1.65×10^{-6}	0.046	0.020	0.100	0.524
64	74.8	76.4	80.7	87.9	3.25×10^{-4}	5.97×10^{-4}	1.54×10^{-5}	2.05×10^{-6}	0.035	0.046	0.130	0.460
68	73.7	77.3	81.1	86.9	4.81×10^{-4}	4.37×10^{-4}	1.39×10^{-5}	2.53×10^{-6}	0.024	0.065	0.151	0.402
72	72.3	77.7	81.3	86.1	8.14×10^{-4}	3.71×10^{-4}	1.32×10^{-5}	3.11×10^{-6}	0.015	0.079	0.166	0.349
76	69.9	78.0	81.4	85.3	1.95×10^{-3}	3.39×10^{-4}	1.30×10^{-5}	3.82×10^{-6}	0.006	0.088	0.174	0.302
78	67.4	78.1	81.4	84.9	4.98×10^{-3}	3.30×10^{-4}	1.30×10^{-5}	4.23×10^{-6}	0.002	0.092	0.177	0.281
80	64.9	78.2	81.4	84.6	1.22×10^{-2}	3.24×10^{-4}	1.31×10^{-5}	4.69×10^{-6}	0.001	0.095	0.179	0.260
82	68.7	78.2	81.4	84.2	2.98×10^{-3}	3.20×10^{-4}	1.32×10^{-5}	5.20×10^{-6}	0.004	0.097	0.180	0.241
84	70.1	78.2	81.4	83.9	1.78×10^{-3}	3.19×10^{-4}	1.34×10^{-5}	5.77×10^{-6}	0.007	0.098	0.180	0.222
90	71.9	78.2	81.2	82.9	9.13×10^{-4}	3.23×10^{-4}	1.41×10^{-5}	7.89×10^{-6}	0.014	0.010	0.177	0.174
98	72.9	78.0	81.0	81.6	6.47×10^{-4}	3.44×10^{-4}	1.56×10^{-5}	1.21×10^{-6}	0.020	0.097	0.168	0.123
100	73.0	78.0	80.9	81.3	6.16×10^{-4}	3.52×10^{-4}	1.60×10^{-5}	1.34×10^{-5}	0.021	0.095	0.165	0.112
106	73.3	77.7	80.6	80.4	5.61×10^{-4}	3.81×10^{-4}	1.76×10^{-5}	1.86×10^{-5}	0.024	0.090	0.155	0.085
110	73.4	77.6	80.4	79.8	5.42×10^{-4}	4.05×10^{-4}	1.88×10^{-5}	2.32×10^{-5}	0.025	0.085	0.148	0.070
120	73.4	77.1	79.9	78.3	5.31×10^{-4}	4.83×10^{-4}	2.24×10^{-5}	4.06×10^{-5}	0.026	0.073	0.128	0.043

local adsorption isotherms as a function of the experimental time is exemplified by using ethylene and propene as probe gases and ZnO, PbO, and $CaCO_3$ as solid adsorbents. Table 1 lists the values of the adsorption parameters ϵ, c^*_{max}, and θ_t for experimental times chosen 2 min apart one from the other, while in Figure 2 the plots of these parameters together with c_y using 3000 plot points are shown.

The appearance of the function $c_y = f(t)$ in Figure 2d is typical for the so-called *diffusion band* of the RF-GC method, i.e., increases initially, passes through a maximum, and then declines with time. As regards the maximum and minimum in the energy function $\epsilon = h(t)$ shown in Figure 2a, these can be attributed to the two partial derivatives $\partial c^*_s/\partial c_y$ and $\partial^2 c^*_s/\partial c_y{}^2$, according to eqs 13 and 15, given the experimental form of $c_y = f(t)$ in Figure 2d. Physically, the gas molecules at time t are not exclusively adsorbed on sites i all of the same energy ϵ_i. Figure 2a shows simply the sweeping effect of the dynamic and changing with time procedure on the sites of various energies, giving rise to transition adsorption energies before their final leveling off with time.

The dependence of adsorption energies on time is not a new finding. For example, Kiselev and Yashin[20] report adsorption energies as "initial" differential heats of adsorption. Their values in the systems C_2H_4/CaZeolite (53.6 kJ/mol) and C_3H_6/CaZeolite (57.3 kJ/mol) seem comparable to the adsoption energy values given in Table 1, ranging between 64.9 and 119.2 kJ/mol. However, this comparison is rather impermissible, since the first refer to global overall values and not to local values as the latter ones. Katsanos et al.[21] found 80.3 kJ/mol for heptane adsorbed on aluminum oxide activated at 440 °C. Besides, the above values[20,21] were calculated for a whole temperature range, whilst in the present case all values refer to a single temperature (50 °C), considerably lower than before.

Although the local relative coverage of the surface θ_t is known to be an increasing function of the equilibrium pressure or concentration and asymptotically tending to unity, the time dependence of the local θ_t is not necessarily analogous, since it does not comprise all sites, but only those active at time t. One can see from Figure 2 that the maximum in ϵ and θ_t appears at the same time as that in c_y. This is expected from eq 10 for θ_t (derived from eq 7) and from eq 15 for ϵ. The value of c^*_{max} depends also on the partial derivatives $\partial c^*_s/\partial c_y$ and $\partial^2 c^*_S/\partial c_y{}^2$, according to eqs 13 and 16, thus explaining its discontinuities

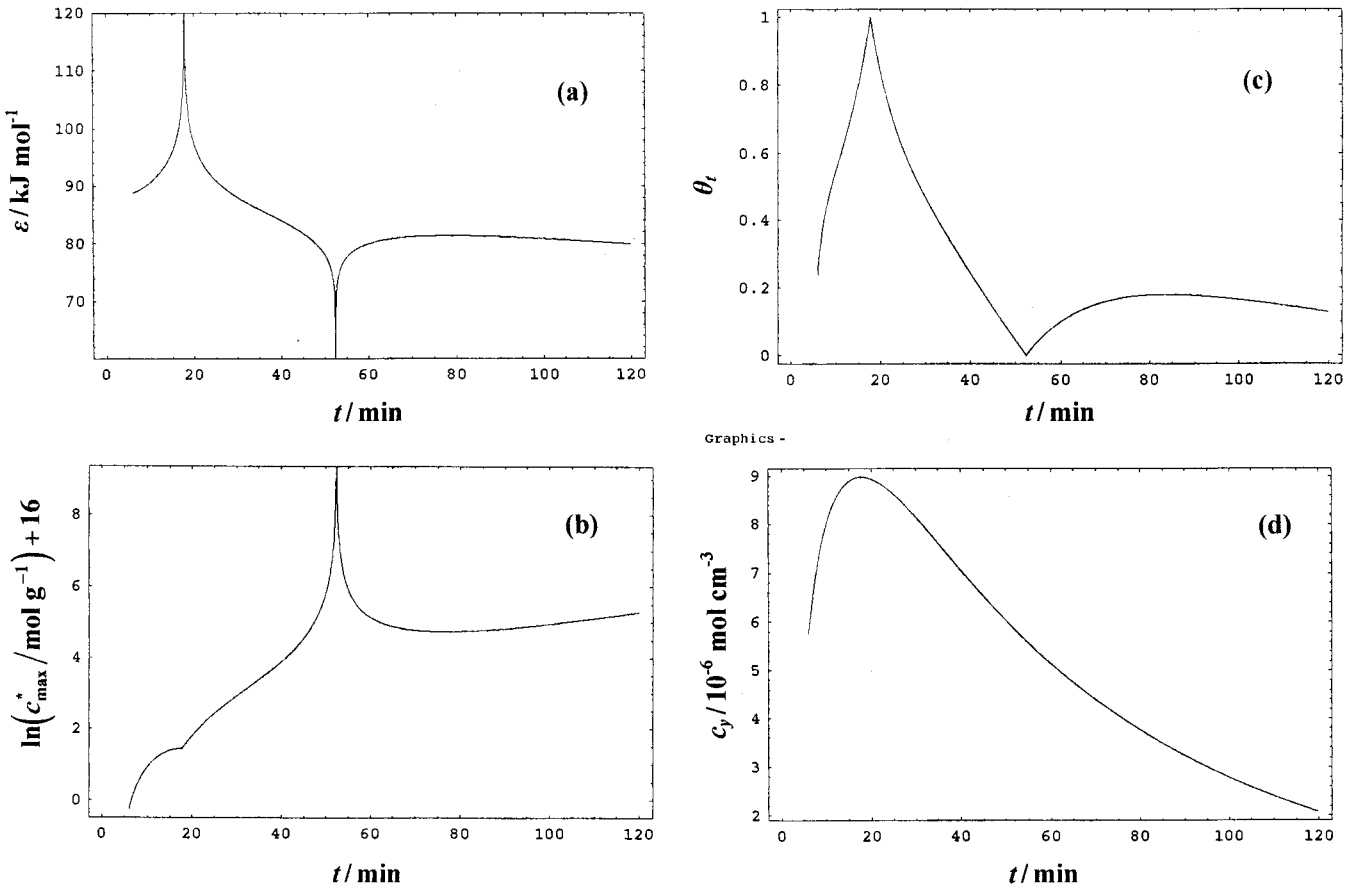

Figure 2. Plots of adsorption energies (a), local monolayer capacities (b), local isotherms (c), and gaseous concentrations (d) as a function of experimental time, at 323.2 K, for the system C_3H_6/PbO in nitrogen atmosphere.

with time. After a certain time, all curves of Figure 2 are practically leveled off.

An evidence that the principles proposed here work is to calculate the local specific surface areas of the solid S (m^2/g) referring to each mean energy value ϵ_i (and therefore to each collection of active sites), by multiplying c^*_{max} of eq 16 by Avogadro's number, N_A, and by the molecular cross sectional area of the adsorbed gas A_m. Using the liquid density of propene (0.5193) and eq 2.64 of Gregg's and Sing's book,[22] one finds for propene $A_m = 28.58$ Å^2. Then, $S = c^*_{max} N_A A_m \times 10^{-20}$ m^2/g. Some values of S from the c^*_{max} values of Table 1 for C_3H_6/PbO, corresponding to a few chosen times, are given below:

t (min)	6	18	28	42	50	52	54	60	120
S (m^2/g)	0.015	0.086	0.298	1.20	6.59	47.9	10.9	3.31	3.86

Since PbO is a rather nonporous material, the values of S seem logical, distributed over the range 0.015−47.9 m^2/g, for the various collections of sites i. Another evidence that θ_t represents a local isotherm is its plot as a function of c_y in Figure 3. It looks like a hysteresis loop of adsorption, but it is not, since the desorption (b) curve lies below that of adsorption (a). The latter corresponds to the ascending branch of Figure 2d, while desorption is connected with the descending branch of c_y. The separation of the desorption (b) from the adsorption (a) curve is most probably due to irreversible adsorption of the adsorbate on the solid surface. As $\theta_t = c_s/c^*_{max}$, an amount x stuck permanently on the adsorption sites makes $\theta'_t = (c^*_s - x)/(c^*_{max} - x)$, which is smaller than θ_t, and this is exactly what is observed experimentally; i.e., at a given c_y, e.g., 7×10^{-6} mol cm^{-3}, realized at two times during the experiment, one

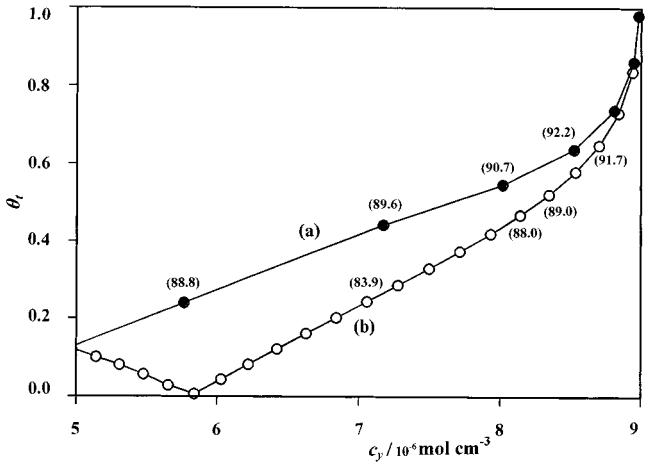

Figure 3. Adsorption (●)/desorption (○) isotherm plots at 323.2 K for the system C_3H_6/PbO in a nitrogen atmosphere. Branch (a) corresponds to the c_y values of the ascending part of Figure 2d, while branch (b) contains the c_y values of the descending part of it. Numbers in parentheses are the energies of adsorption ϵ (kJ/mol) taken from Table 1.

corresponds to θ_t and the other to θ'_t. The extent of irreversibly adsorbed analyte can be calculated as described elsewhere.[10]

The magnitude range of the adsorption energies points to a rather regular distribution model for the adsorption sites on heterogeneous surfaces, in the domain of chemisorption. The adsorption energy ϵ increasing with θ_t up to a maximum close to unity for the latter confirms that different collections of adsorption sites are involved at different times.

The kinetic physicochemical quantities pertaining to the adsorption phenomenon are given in Table 2, placed in the

Supporting Information. Any functional relation between ϵ, c^*_{max}, and θ_t and these quantities would be rather premature at the present stage. Premature also is the comparison of the adsorption energy values of Table 1 with the rate constants of Table 2, the first being based on local equilibration of the probe gases (C_2H_4 and C_3H_6) with the solid surface and the latter being pure kinetic parameters. Using the microscopic reversibility equilibrium distribution constant $K = k_1/k_{-1}$, one can calculate the adsorption energy ϵ with the help of eq 8, i.e., via a considerably different path than that of eq 15. The results at 323.2 K are as follows (in kJ/mol): C_2H_4/ZnO (73.6); C_2H_4/PbO (94.5); C_3H_6/PbO (70.4); C_3H_6/$CaCO_3$ (70.4). Only in the first case does the value of 73.6 coincide with the long time value of Table 1 (73.4).

More experimental results and other additional adsorption properties, like probability density functions with respect to the energies, are required to reach acceptable conclusions. The above additional work is well under way.

Acknowledgment. The generous help of Mrs. M. Barkoula and Miss A. Malliori is gratefully acknowledged by the authors.

Supporting Information Available: The Compact PC program in GW-BASIC, for calculating directly from the experimental pairs *H*, *t* the various adsorption and kinetic physicochemical parameters, and Table 2. This information is available free of charge via the Internet at http://pubs.acs.org.

References and Notes

(1) Katsanos, N. A.; Thede, R.; Roubani-Kalantzopoulou, F. *J. Chromatogr. A* **1998**, *795*, 133.

(2) Roles, J.; Guiochon, G. *J. Chromatogr*. **1992**, *591*, 233.

(3) Stanley, B.; Guiochon, G. *J. Phys. Chem*. **1993**, *97*, 8098.

(4) Golshan-Shirazi, S.; Guiochon, G. *J. Chromatogr*. **1994**, *670*, 1.

(5) Stanley, B. J.; Guiochon, G. *Langmuir* **1994**, *10*, 4278; **1995**, *11*, 1735.

(6) Quinones, I.; Guiochon, G. *J. Colloid Interface Sci.* **1996**, *183*, 57.

(7) Heuchel, M.; Jaroniec, M.; Gilpin, R. K. *J. Chromatogr*. **1993**, *628*, 59.

(8) Abatzoglou, Ch.; Iliopoulou, E.; Katsanos, N. A.; Roubani-Kalantzopoulou, F.; Kalantzopoulos, A. *J. Chromatogr*. *A* **1997**, *775*, 211.

(9) Katsanos, N. A.; Dalas, E. *J. Phys. Chem*. **1987**, *91*, 3103.

(10) Sotiropoulou, V.; Vassilev, G. P.; Katsanos, N. A.; Metaxa, H.; Roubani-Kalantzopoulou, F. *J. Chem. Soc., Faraday Trans*. **1995**, *91*, 485.

(11) Jovanovic, D. S. *Colloid Polym. Sci.* **1969**, *235*, 1203, 1214.

(12) Fowler, R.H. *Statistical Mechanics*, 2nd ed.; Cambridge University Press: Cambridge, U.K., 1936; p 829.

(13) Hazlett, J. D.; Hsce, C. C.; Wojciechowski, B. W. *J. Chem. Soc., Faraday Trans. 2* **1979**, *75*, 602.

(14) Rudzinski, W.; Wojciechowski, B. W. *J. Colloid Polym. Sci.* **1977**, *255*, 869, 1086.

(15) Sircar, S. *J. Colloid Interface Sci.* **1984**, *101*, 452.

(16) Jaroniec, M.; Sokolowski, S.; Waksmundzki, A. *Pol. J. Chem.* **1976**, *50*, 779.

(17) Rudzinski, W.; Everett, D. H. *Adsorption of Gases on Heterogeneous Surfaces*; Academic Press: London, 1992; pp 452−456.

(18) Landman, U.; Montroll, E. W. *J. Chem. Phys.* **1976**, *64*, 1762.

(19) Katsanos, N. A.; Karaiskakis, G. *J. Chromatogr*. **1987**, *395*, 423.

(20) Kiselev, A. V.; Yashin, I. *Gas Adsorption Chromatography*; Plenum: New York, 1969; p 47.

(21) Katsanos, N. A.; Lycourghiotis, A.; Tsiatsios, A. *J. Chem. Soc., Faraday Trans. 1* **1978**, *74*, 575.

(22) Gregg, S. J.; Sing, K. S. W. *Adsorption, Surface Area and Porosity*; Academic Press: London, 1967; p 67.